

Journal of Materials Chemistry B

Accepted Manuscript



This is an *Accepted Manuscript*, which has been through the Royal Society of Chemistry peer review process and has been accepted for publication.

Accepted Manuscripts are published online shortly after acceptance, before technical editing, formatting and proof reading. Using this free service, authors can make their results available to the community, in citable form, before we publish the edited article. We will replace this *Accepted Manuscript* with the edited and formatted *Advance Article* as soon as it is available.

You can find more information about *Accepted Manuscripts* in the [Information for Authors](#).

Please note that technical editing may introduce minor changes to the text and/or graphics, which may alter content. The journal's standard [Terms & Conditions](#) and the [Ethical guidelines](#) still apply. In no event shall the Royal Society of Chemistry be held responsible for any errors or omissions in this *Accepted Manuscript* or any consequences arising from the use of any information it contains.

Cite this: DOI: 10.1039/c0xx00000x

www.rsc.org/xxxxxx

ARTICLE TYPE

Multifunctional Water-Soluble Luminescent Carbon Dots for Imaging and Hg²⁺ Sensing†

Yanling Zhai, Zhijun Zhu, Chengzhou Zhu[‡], Jiangtao Ren, Erkang Wang and Shaojun Dong**Received (in XXX, XXX) Xth XXXXXXXXX 20XX, Accepted Xth XXXXXXXXX 20XX*

DOI: 10.1039/b000000x

We propose an ingenious method for large-scale fabrication of water-soluble photoluminescent carbon dots (CDs) by a one-step microwave route in the presence of citric acid and ethylenediamine. In contrast to other CDs-based nanomaterials, the prepared CDs exhibit highly fluorescent quantum yield (QY) and excellent stability in both organic and inorganic phases. After simple post-treatments, CDs can be used as a new type of fluorescent ink for information storage and nanofibers electrospinning. It should be noted that the CDs are the superior fluorescent bioimaging agent in cell, plants and animals according to their excellent solubility and ultra-low toxicity. In addition, the CDs could be utilized as a modification-free biosensor reagent capable of detecting Hg²⁺ in complex environments. More significantly, environmental friendly “skillful pens” were fabricated, and they also provided an effective platform for portable qualitative-detection of Hg²⁺.

1. Introduction

Photoluminescent carbon dots (CDs), as one of new members of carbon nanomaterials family, have drawn considerable attention owing to their promising advantages.¹⁻⁶ In comparison to conventional organic dyes and semiconductor quantum dots (QDs), which have raised serious healthy and environmental concerns, the CDs are remarkably advantageous in their green synthesis, high aqueous solubility, robust chemical inertness, easy functionalization, high resistance to photobleaching and low cytotoxicity.^{3, 7} CDs hold great promise in a wide range of technologies, such as bioimaging,⁸⁻¹⁰ catalysis,^{11, 12} sensing,^{13, 14} and other different optoelectronic device applications.^{15, 16} However, with the exception of promising commercial applications, photoluminescence (PL) properties of CDs from solid states are still not satisfactory because of their low quantum yield (QY) or strong fluorescence quenching in dry and aggregate states. Routes to synthesize CDs can be classified into two main categories: top-down and bottom-up methods. The former are based on post-treating of nanocarbon broken from various larger carbon structures, while bottom-up methods include thermal decomposition, combustion and dehydration of suitable molecular precursors.¹⁷ Generally, these methods involve intricate processes and severe synthetic conditions, and the QY of obtained CDs is very low with only a few exceptions. More recently, microwave pyrolysis of carbohydrates solution has become more and more popular because of the low cost and simple synthesis.¹⁸⁻²⁰ However, to achieve highly luminescent CDs, surface-passivation reagents are usually required.^{15, 21, 22} Microwave pyrolysis of different carbohydrates either in the presence or absence of any surface passivating agent and dehydration of carbohydrates with subsequent surface passivation

have been reported to produce C-dots with sufficient QY. Maybe because the high reaction temperature, not increasing from low temperature to high temperature slowly, the polymer-like CDs could change to carbogenic CDs rapidly, which produce the satisfactory CDs. Moreover, too much attention has still been paid to their applications in biological labelling, bioimaging or drug delivery. In principle, of particular interest and significance are the findings that CDs in the solid states can exhibit strong PL emission and the PL from CDs can be quenched efficiently by either electron acceptor or electron donor molecules in solution. Therefore, exploring efficient strategies for the large-scale fabricating of CDs with high QY and further expanding their novel applications are still a challenge.

Herein, using citric acid and ethylenediamine as precursors, a one-step microwave synthesis of CDs with high QY on a large scale is reported. The morphology and chemical structures are investigated extensively. Compared to the currently available CDs-based nanomaterials, our strategies for the fabricating of CDs hold great promise in their synthesis and applications. The benefits are as follows: 1) simple synthesis, only required microwave irradiation for 5 min; 2) low-cost and large-scale fabrication, thus the potential for industrial production; 3) strong fluorescence in dry and aggregate states, hence ensuring its innovative applications in patterning and information storage; 4) high QY (41.39%) without any modifier/surface passivated agent, excellent water-solubility and stability and good biocompatibility, therefore utilized as fluorescent bioimaging agents in cells, plants and animals; 5) efficient PL quenching by Hg²⁺ ions, providing particularly useful platform for portable detection of Hg²⁺ in complex environments.

2. Results and discussion

Our strategy for the fabrication of CDs was detailedly described in the Supporting Information. The transmission electron microscopy (TEM) images showed that the synthesized CDs were highly monodisperse (Figure S1) and narrowly distributed with diameters in the range of 2.5 ± 0.5 nm (Figure 1A and inset). A typical X-ray diffraction (XRD) pattern of CDs displays a broad diffraction peak located around 18.5° (Figure S2), suggesting an amorphous nature, which is consistent with the discernible lattice structures from the HRTEM image (data not shown). To probe the chemical composition and content of the as-produced CDs, X-ray photoelectron spectroscopic (XPS) measurements were implemented. As shown in Figure 1B, the survey spectra of CDs samples revealed the presence of C, N and O, as well as limited H (4%, calculated) without any other impurities. In detail, the C1s spectrum (inset) were deconvoluted into three peaks at 284.75, 286.15, and 287.7 eV, which are attributed to C–C/C=C, C–O, and C–N, respectively.²³ What's more, sp²- and sp³-hybridized carbon atoms were distinguished from ¹³C NMR spectroscopy (Figure 1C), and ¹H NMR spectrum (Figure S3).²⁴ In addition, Fourier Transform Infrared Spectroscopy (FT-IR) spectra were recorded to identify the functional groups on CDs. As shown in Figure 1D, the strong peaks at 1650 cm⁻¹, 1570 cm⁻¹, 1435 cm⁻¹ and 1291 cm⁻¹ are attributed to C=O, N-H, CH₂ and C-N, respectively. The broad band centered at 3276 cm⁻¹ suggested the existence of -OH and N-H, which improve the hydrophilicity and stability of the CDs in aqueous system.²³ The UV-vis absorption and PL emission spectra of the as prepared CDs were also investigated in Figure 1E. The absorption spectrum showed a narrow peak at 349 nm and the optimal excitation and emission wavelengths were located at 360 nm and 455 nm, indicating the narrow size distribution of CDs as well. The photograph of the CDs dispersion under UV light (365 nm) exhibited a blue color (inset), further revealing that the resultant CDs exhibit blue fluorescence.

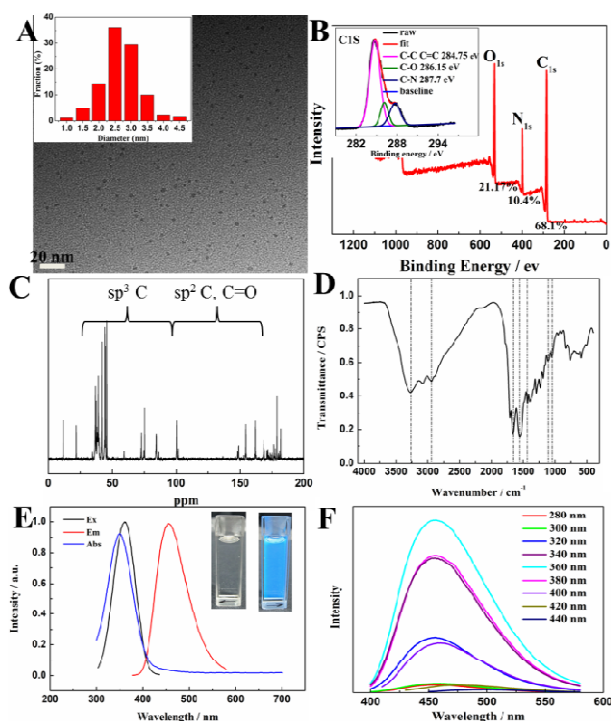


Figure 1. (A) HRTEM image and size distribution (inset) of the synthesized CDs; scale bar: 20 nm. (B) XPS of CDs (inset: C1s spectra). (C) ¹³C-NMR and (D) FTIR spectra of the CDs. (E) UV/Vis absorption, PL excitation and emission spectra, and (inset) photographs of the CDs under room light (left) and UV light (right) in aqueous solution. (F) Excitation-dependent PL spectra of the CDs in aqueous solution.

To further explore the optical properties of the as-prepared CDs, the excitation-dependent PL behavior was carried in Figure 1F. Unlike most other luminescent CDs,^{25, 26} the PL peak of the resultant CDs remained unchanged, while exhibited an excitation-dependent PL behavior for the excitation wavelength exceeding 400 nm, indicating the relatively uniform and well-passivated CD surface. Furthermore, the effects of reaction conditions on the QY of CDs were investigated. Microwave irradiation time was critical to PL of the synthesized CDs, as the reaction time progressed from 4 min to 15 min (Table S1), the PL QYs could reach up to 41.39 % under the optimized reaction conditions (5 min), which is much higher than those of most recorded fluorescent carbon-based materials.¹⁹ Besides high QY, the prepared CDs exhibited excellent stability, which is essential for practical applications. The PL intensity of CDs remained constant in a wide pH (3–11) of solutions dispersion in aqueous solution (Figure S4) and also in DMF solution. In addition, these nanoparticles could be well-dispersed in kinds of solvents without any detectable agglomeration, and there were no changes in colour and PL intensities after exposure to room light for more than one month (Figure S5). The preminent PL of CDs makes the feature of their great potential applications, which will be discussed in the next section.

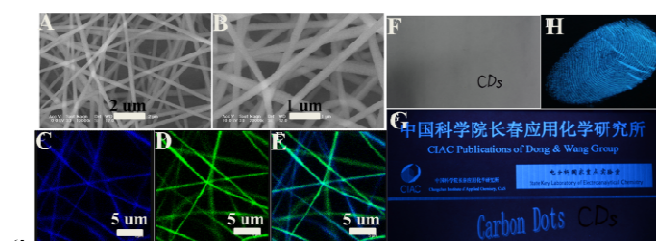


Figure 2. SEM (A and B) and fluorescent images (C-E) of CNFs captured in exciter filter wavelengths of (C) 365 nm, (D) 488 nm and (E) overlay of C and D. Digital photographs of the filter paper printed with CDs ink under (F) room light and (G) a UV hand lamp (365 nm). The marked letters “CDs” were written with an ordinary pen. (H) A CDs-formed fluorescent fingerprint on filter paper captured under a UV hand lamp.

To make full use of the high QY, the CDs were utilized to prepare carbon nanofibers (CNFs) by electrospinning CDs solution with the aid of polymers. As observed from SEM images (Figure 2A and B), the prepared CNFs lengthed up to tens of micrometers, showing high aspect ratios and an average diameter of 300 nm (Figure S6). Under ultraviolet (365 nm) and blue (488 nm) light excitation, CNFs exhibited blue (Figure 2C) and green (Figure 2D) luminescence, respectively, and they overlapped very well (Figure 2E). In addition, the water-soluble CDs were also available as a fluorescent agent for daily work. After simple post-treatments, CDs have been employed as a new type of biocompatible fluorescent ink. Multiple words and images were printed on a filter paper marked with “CDs” letters written with an ordinary pen, which were invisible under ambient light (Figure 2F). However, these patterns could be clearly revealed under UV

light (Figure 2G). Notably, being exposed under ambient light for two months, the fluorescent properties of the products exhibited no significant changes (Figure S7). Furthermore, the CDs could be used as inkpad. As shown in Figure 2H, a fluorescent CDs fingerprint was printed on filter paper, which could reflect human's fingerprint discriminately and clearly. Compared with traditional inks, the water-soluble CDs inks are clear, permanent, adomorphonic, pollution-free, and easy to clean with water, which provides a new way to feed the potential requirement on a commercial scale.

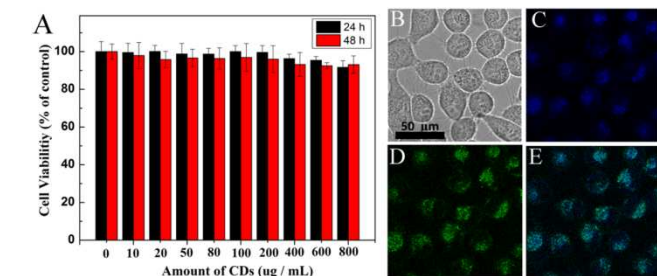


Figure 3. (A) Cytotoxicity testing results of CDs on HeLa cells viability. The values represent percentage cell viability (means \pm SD, n=6). (B-E) Laser scanning confocal microscopy images of CDs to HeLa cells. The samples were observed under (B) bright field and excited at (C) 405 nm, (D) 488 nm and (E) overlay of C and D.

These encouraging results prompted us to evaluate the feasibility of CDs as a new fluorescent marker for living cell imaging.²⁷ For effective bioimaging, it is required that the selected fluorescent marker has not only optical merits but also low cytotoxicity.²⁸ To evaluate the cytotoxicity of CDs, the viability of HeLa cells treated with CDs was measured by the methyl thiazolyl tetrazolium (MTT) method. As shown in Figure 3A, HeLa cells were incubated with different doses of CDs for 24 and 48 h, respectively. Subsequently, the viability remained greater than 90% even incubated with ultrahigh concentration (800 µg/mL) of CDs for 48 h, demonstrating instinctively low toxicity of the CDs (without any further functionalization).²⁹ Figure 3B displays photographs of the HeLa cells captured by a laser scanning confocal microscope. It is obvious that the transfected HeLa cells became quite bright owing to the strong fluorescence from CDs, indicating a large amount of CDs have been internalized into the cells (Figure S8). Consistent with fluorescence microscopy assay results, bright blue (Figure 3C) and green (Figure 3D) fluorescence could be observed under ultraviolet and blue light excitation, and the two-channel luminescence images for the same scanning area overlapped well (Figure 3E). This multicolour emission shows a great advantage of the CDs over other labelling agents, because it gives us much space to choose the wavelength for observation *in vitro*.

Given the low cytotoxicity, we further tested the toxicity and feasibility of CDs as bioimaging agents in both plants and animals. Firstly, some selected mung beans were raised in aqueous solution of CDs (4 mg/mL) at constant-temperature bath (23 °C). Similar to bean sprouts grown in water (Figure S9), no abnormal sprouts were found after three days grown in aqueous solution of CDs (Figure 4A). Under a UV hand lamp, sprouts exhibited strong characteristic blue luminescence from CDs, which illustrated that CDs could permeate throughout the plant cells, and had no perceptible effect on plant growth (Figure 4B).

The potential value of CDs as luminescent probes for *in vivo* imaging was then carried out on mice. The dorsum was shaved for fluorescence detection of the CDs trapped in organs. An aliquot (100 µL) of CDs dispersed in water was subcutaneously injected into a mouse (Figure 4C). From Figure 4D, a bright emission was clearly visible at the injection site, which has also been detected from HeLa cells and sprouts treated with CDs, thereby revealing that the application of CDs could be extended to *in vitro* fluorescence imaging. For the intravenous injection, 100 µL CDs solution was also injected into mice. During the whole-body circulation, no obvious emission was observed in dorsum. As shown in Figure 4E, after 2 h postinjection, bright fluorescence in the urine was visible, while the observed fluorescence got generally weak at 4 h post-intravenous injection, suggesting a low accumulation level of the CDs (Figure 4F, corresponding spectrum given in Figure S10). These results suggest the injected CDs without the modifier/surface passivated agent can excrete via urine easily, and have no obvious toxicity as bioimaging materials *in vivo*. The mechanism for rapid and efficient urinary excretion and elimination of QDs (hydrodynamic diameter < 5.5 nm) from the body has been investigated detailedly by Frangioni's group.³⁰

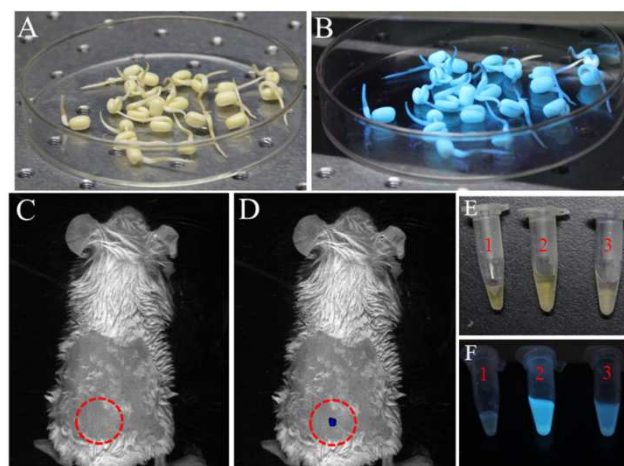


Figure 4. Optical and fluorescent images of bean sprouts grown with CDs aqueous solution (4 mg/mL) under (A) daylight and (B) 365 nm excitation. (C) Bright field and (D) as-detected fluorescence of mice through subcutaneous injection of CDs. PL spectra of the urine of mice under (E) daylight and (F) 365 nm excitation: (1) without injection CDs aqueous; (2, 3) after injection of CDs aqueous solution for (2) 2 h and (3) 4 h.

Heavy-metal ions, such as mercury and lead, can cause serious and permanent damage to human organs due to their accumulative characters in the environment and biota.^{31, 32} Therefore, detection of these heavy-metal ions is central to the environmental monitoring of water or soil.³³

Of particular interest and significance is the finding that the prepared CDs can be utilized as a highly efficient nanoprobe for Hg²⁺ detection. Figure 5A shows the fluorescent quenching value of CDs with increased Hg²⁺ concentration, and the inset shows the linear relationship between PL intensity and Hg²⁺ concentration. The detection limit was calculated to be 20 nmol/L, which is lower than the acceptable Hg²⁺ concentration in drinking water (0.006 mg/mL) according to the World Health Organization (WHO).³⁴ Besides sensitivity, selectivity is another

important parameter to evaluate the performance of the sensing system. We then investigated the effect of representative metal ions (Cd^{2+} , Fe^{2+} , Ag^+ , Pb^{2+} , Fe^{3+} , Cr^{2+} , Mg^{2+} , Ca^{2+} , Na^+ , K^+ , Co^{2+} , Zn^{2+} , Mn^{2+} , Cu^{2+} and Hg^{2+}) on CDs fluorescence quenching under the same conditions. As shown in Figure 5B, most of those metal ions of ultrahigh concentrations (0.2 mmol/L), can not induce obvious fluorescence decreases of CDs except for Fe^{3+} ions. Fortunately, in the valid range for Hg^{2+} detection from 0 to 3 μM (Figure S12 A), no obvious fluorescence quenching took place in the present of Fe^{3+} ions (Figure S11). These results validate the high efficiency of our nanoprobe to detect Hg^{2+} in water. However, a much more challenging goal is to detect Hg^{2+} in real samples, since many of the current nanoprobe are not stable enough when used in a complicated environment.

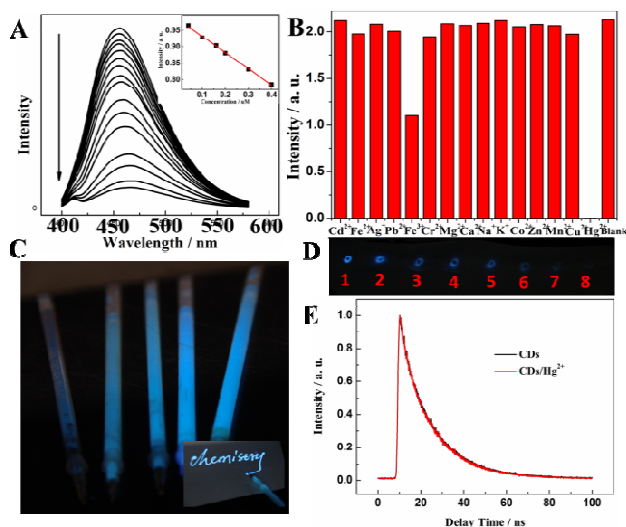


Figure 5. (A) Fluorescence quenching of CDs in the presence of Hg^{2+} ions (0–60 μM). (B) Comparison of fluorescence intensities of CDs after the addition of Hg^{2+} ions (20 μM) and other different metal ions (200 μM), respectively. (C) Optical images of the colorful rollerball pens loaded with different concentration CDs inks. (Inset: the fluorescent text written on a filter paper under a UV hand lamp). (D) The photograph of ring on filter paper written with different amount of Hg^{2+} (from 1 to 8: 0, 30 nM, 100 nM, 300 nM, 500 nM, 1 μM , 30 μM , and 50 μM) under a UV hand lamp. (E) Fluorescence decay of CDs without and with Hg^{2+} (0.02 mM) as a function of time (375 nm excitation, delay time at 455 nm emission).

To evaluate the practicality of this sensor, we applied a standard addition method to detect Hg^{2+} in lake water obtained from the South Lake of Changchun. On the basis of the ICP-OES, after addition of 40, 60, 100, 160 nM Hg^{2+} in lake water, the recoveries were 102.5%, 98.2%, 96.1% and 99.2%, respectively (Table S2), which indicated the accuracy and reliability of our nanoprobe for Hg^{2+} determination in environmental samples. To realize facile use of this nanoprobe, portable Hg^{2+} -responsive rollerball pens were developed. It was noteworthy that the prepared rollerball pens loaded with different concentrations of CDs inks exhibited multicolour luminescence (Figure 5C) and could readily flow during writing without leakage or coagulation within the pen (inset), therefore might replace commercial coloured pens, which are of high toxicity. As observed in Figure 5D, eight homology rings were written on common filter paper (or any other substrates without autofluorescence) with one of the pens, and the color of the rings changed to light blue gradually,

and then to colorless with the addition of Hg^{2+} . Compared with other test papers reported, our fabricated “skillful pen” had great superiority in Hg^{2+} determination—they are environmental friendly, affordable, portable and easy-to-operate for real-time monitoring. Finally, the decay dynamics was measured to investigate the PL quenching mechanism of this system. As shown in Figure 5E, the lifetime contains two lifetime components, 3.4 ns and 15.5 ns for CDs, and 3.6 ns and 15.4 ns for CDs/ Hg^{2+} , meaning the same average lifetime for the CDs before and after coordination with Hg^{2+} ions, which demonstrated no nonradiative electron-transfer happening during PL quenching progress.³⁵ The energy state of Hg^{2+} complex in the coordinated ions may be influenced by the nature of the CDs, and fluorescent quenching of CDs would be due to the selective absorption of light by the Hg^{2+} atom. At the same time, we found that the maximum emission peaks of CDs located at 455 nm gradually red-shift to 466 nm with varying concentrations of Hg^{2+} (Figure S11B). These results indicate the special coordination interaction between Hg^{2+} ions and the phenolic hydroxyl groups of the CDs contribute to the quenching progress, which has been used for the detection of metal ions or colored reactions in traditional organic chemistry.³⁶

Acknowledgements

This work was supported by the National Natural Science Foundation of China (No. 21375123) and 973 Project (Nos. 2011CB911002 and 2010CB933603). Y. L. Zhai and Z. J. Zhu contribute equally to this work.

3. Conclusions

In summary, we developed a one-step microwave route for large-scale fabrication of water-soluble CDs. The morphology and chemical structures have been investigated extensively. In comparison with reported CDs-based nanomaterials, the prepared CDs exhibit highly fluorescent QY and excellent stability in both organic and inorganic phases, therefore can be used as a new type of fluorescent ink for information storage and nanofibers electrospinning. A particularly attractive feature of the prepared CDs is their excellent solubility and ultra-low toxicity, empowering the CDs promising use *in vitro*, plants and vivo imaging. It should be noted that the CDs could be utilized as a modification-free biosensor reagent capable of detecting Hg^{2+} in complex environments, and has a remarkable selectivity over representative metal ions. More significantly, environmental friendly “skillful pens” were fabricated, and they also provided an effective platform for portable qualitative-detection of Hg^{2+} . Investigations on the distinct PL properties and luminescent quenching mechanisms of CDs in the present of Hg^{2+} ions are still underway.

Notes and references

State Key Laboratory of Electroanalytical Chemistry, Changchun Institute of Applied Chemistry, Chinese Academy of Sciences, Changchun, Jilin, 130022 China. Tel: +86-431-85262101; Fax: +86-431-85689711. E-mail: dongsj@ciac.ac.cn

†Electronic Supplementary Information (ESI) available: [Experimental sections, TEM, XRD, NMR and fluorescence characterization, digital

- photographs, spectra, QY of the CDs, recovery data for the determination of Hg²⁺ in lake water]. See DOI: 10.1039/b000000x/
‡Present address: Department of Chemistry and Food Chemistry, Dresden University of Technology Bergstraße 66b, 01069 Dresden, Germany.
1. L. Bao, Z. L. Zhang, Z. Q. Tian, L. Zhang, C. Liu, Y. Lin, B. Qi and D. W. Pang, *Adv Mater*, 2011, **23**, 5801-5806.
 2. N. M. Iverson, P. W. Barone, M. Shandell, L. J. Trudel, S. Sen, F. Sen, V. Ivanov, E. Atolia, E. Farias, T. P. McNicholas, N. Reuel, N. M. Parry, G. N. Wogan and M. S. Strano, *Nature nanotechnology*, 2013, **8**, 873-880.
 3. H. Li, Z. Kang, Y. Liu and S.-T. Lee, *J Mater Chem*, 2012, **22**, 24230-24253.
 4. B. Qin, Z. Zhao, R. Song, Z. Tang, *Angew. Chem. Int. Ed.* 2008, **47**, 9875-9878
 5. X. Li, Y. Zhou, Z. Zheng, S. Liu, Z. Tang, *Langmuir*, 2009, **25**, 6580-6586.
 6. J. Zong, Y. Zhu, X. Yang, J. Shen and C. Li, *Chem Commun*, 2011, **47**, 764-766.
 7. Y. Fang, S. Guo, D. Li, C. Zhu, W. Ren, S. Dong and E. Wang, *ACS Nano*, 2012, **6**, 400-409.
 8. L. Cao, X. Wang, S.-Y. Xie and Y.-P. Sun, *J Am Chem Soc*, 2007, **129**, 11318-11319.
 9. S. T. Yang, L. Cao, P. G. Luo, F. Lu, X. Wang, H. Wang, M. J. Mezziani, Y. Liu, G. Qi and Y. P. Sun, *J Am Chem Soc*, 2009, **131**, 11308-11309.
 10. S. T. Yang, X. Wang, H. F. Wang, F. S. Lu, P. J. G. Luo, L. Cao, M. J. Mezziani, J. H. Liu, Y. F. Liu, M. Chen, Y. P. Huang and Y. P. Sun, *J Phys Chem C*, 2009, **113**, 18110-18114.
 11. Y. Li, Y. Zhao, H. Cheng, Y. Hu, G. Shi, L. Dai and L. Qu, *J Am Chem Soc*, 2012, **134**, 15-18.
 12. Z. Xie, F. Wang and C.-y. Liu, *Adv Mater*, 2012, **24**, 1716-1721.
 13. S. Liu, J. Tian, L. Wang, Y. Zhang, X. Qin, Y. Luo, A. M. Asiri, A. O. Al-Youbi and X. Sun, *Adv Mater*, 2012, **24**, 2037-2041.
 14. W. Shi, X. Li and H. Ma, *Angew Chem Int Ed*, 2012, **51**, 6432-6435.
 15. F. Wang, Z. Xie, H. Zhang, C.-y. Liu and Y.-g. Zhang, *Adv Funct Mater*, 2011, **21**, 1027-1031.
 16. X. Yan, X. Cui, B. Li and L. S. Li, *Nano Lett*, 2010, **10**, 1869-1873.
 17. S. N. Baker and G. A. Baker, *Angew Chem Int Ed*, 2010, **49**, 6726-6744.
 18. A. Jaiswal, S. S. Ghosh and A. Chattopadhyay, *Chem Commun*, 2012, **48**, 407-409.
 19. X. Zhai, P. Zhang, C. Liu, T. Bai, W. Li, L. Dai and W. Liu, *Chem Commun*, 2012, **48**, 7955-7957.
 20. H. Zhu, X. Wang, Y. Li, Z. Wang, F. Yang and X. Yang, *Chem Commun*, 2009, 5118-5120.
 21. X. Wang, L. Cao, S. T. Yang, F. Lu, M. J. Mezziani, L. Tian, K. W. Sun, M. A. Bloodgood and Y. P. Sun, *Angew Chem Int Ed*, 2010, **49**, 5310-5314.
 22. Y. Yang, J. Cui, M. Zheng, C. Hu, S. Tan, Y. Xiao, Q. Yang and Y. Liu, *Chem Commun*, 2012, **48**, 380-382.
 23. S. Qu, X. Wang, Q. Lu, X. Liu and L. Wang, *Angew Chem Int Ed*, 2012, **51**, 12215-12218.
 24. S. Zhu, Q. Meng, L. Wang, J. Zhang, Y. Song, H. Jin, K. Zhang, H. Sun, H. Wang and B. Yang, *Angew Chem Int Ed*, 2013, **52**, 3953-3957.
 25. S. Mitra, S. Chandra, T. Kundu, R. Banerjee, P. Pramanik and A. Goswami, *RSC Advances*, 2012, **2**, 12129.
 26. C. Z. Zhu, J. F. Zhai and S. J. Dong, *Chem Commun*, 2012, **48**, 9367-9369.
 27. C. Liu, P. Zhang, X. Zhai, F. Tian, W. Li, J. Yang, Y. Liu, H. Wang, W. Wang and W. Liu, *Biomaterials*, 2012, **33**, 3604-3613.
 28. Y. P. Sun, B. Zhou, Y. Lin, W. Wang, K. A. Fernando, P. Pathak, M. J. Mezziani, B. A. Harruff, X. Wang, H. Wang, P. G. Luo, H. Yang, M. E. Kose, B. Chen, L. M. Veca and S. Y. Xie, *J Am Chem Soc*, 2006, **128**, 7756-7757.
 29. C. Ding, A. Zhu and Y. Tian, *Accounts Chem Res*, 2013, **47**, 20-30.
 30. H. S. Choi, W. Liu, P. Misra, E. Tanaka, J. P. Zimmer, B. Itty Ipe, M. G. Bawendi and J. V. Frangioni, *Nat Biotechnol*, 2007, **25**, 1165-1170.
 31. Y. Long, D. Jiang, X. Zhu, J. Wang and F. Zhou, *Anal Chem*, 2009, **81**, 2652-2657.
 32. C. Zong, X. Liu, H. Sun, G. Zhang and L. Lu, *J Mater Chem*, 2012, **22**, 18418.
 33. Y. L. Liu, K. L. Ai, X. L. Cheng, L. H. Huo and L. H. Lu, *Adv Funct Mater*, 2010, **20**, 951-956.
 34. D. B. Liu, W. S. Qu, W. W. Chen, W. Zhang, Z. Wang and X. Y. Jiang, *Anal Chem*, 2010, **82**, 9606-9610.
 35. M. a. T. Fernandez-Argluelles, A. Yakovlev, M. Oheim and W. J. Parak, *Nano Lett*, 2007, **7**, 2613-2617.
 36. E. F. Wesp and W. R. Brode, *J Am Chem Soc*, 1934, **56**, 1037-1042.

ToC figure

5

